

PAPER • OPEN ACCESS

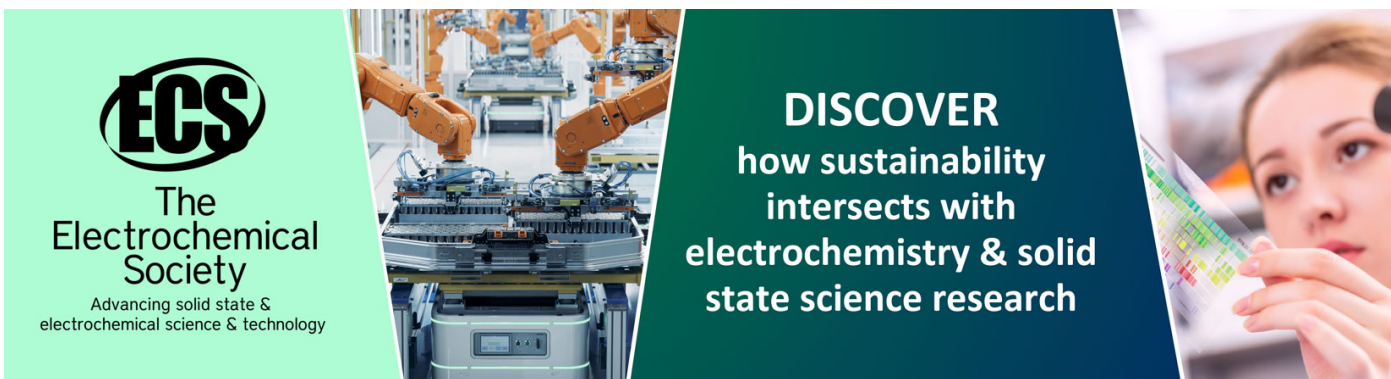
An Efficient Method for Density Projection Field Solution Based on Finite Element Method

To cite this article: Zhengyu Zhang *et al* 2020 *J. Phys.: Conf. Ser.* **1624** 032025

View the [article online](#) for updates and enhancements.

You may also like

- [New AlGaIn/GaN HEMTs employing both a floating gate and a field plate](#)
Jiyong Lim, Young-Hwan Choi, Young-Shil Kim *et al.*
- [ReconU-Net: a direct PET image reconstruction using U-Net architecture with back projection-induced skip connection](#)
Fumio Hashimoto and Kibo Ote
- [A 9 T SRAM cell with data-independent read bitline leakage and improved read sensing margin for low power applications](#)
Adeeba Sharif, Sayeed Ahmad and Naushad Alam



ECS
The
Electrochemical
Society
Advancing solid state &
electrochemical science & technology

DISCOVER
how sustainability
intersects with
electrochemistry & solid
state science research

An Efficient Method for Density Projection Field Solution Based on Finite Element Method

Zhengyu Zhang¹, Fushun Zhu², Run Zhou¹, Qinmei Chen^{2,*} and Hua Yan²

¹China Aerodynamics Research and Development Center, Mianyang, China

²College of Electronics and Information Engineering, Sichuan University, Chengdu China

*Corresponding author email: 2018222050200@stu.scu.edu.cn

Abstract. In the wind tunnel flow field, the relationship between the density projection field, caused by disturbance, and the offset angle of light meets the Poisson equation. However, the source term of the Poisson equation is composed of a series of measured offset angles, which makes it can not be solved effectively by the existing methods. On the basis of the finite element method (FME), we established the fitting formula between the offset angles in the source terms and their corresponding coordinates by employing the Genetic algorithms and back-propagation (GA-BP) neural network. Meanwhile, when the element load vectors were solved, the double integral expression of the entire triangle element prediction was approximately replaced by the constant expression of the triangle vertex element prediction. Simulation experiments demonstrate that compared with the traditional interpolation, the neural network can achieve higher fitting precision. And the proposed algorithm greatly improves the operation speed under the same solution error. By applying the proposed algorithm to the real flow field, the obtained features of the density field are similar to those obtained in the real environment. These imply that the proposed method provides a new useful tool for the study of the density projection field.

Keywords: Density projection field; Poisson equation; GA-BP; FME.

1. Introduction

The density projection field information of the physical model in the wind tunnel flow field is critical data for the aerodynamic shape optimization of aircraft. Therefore, a quantitative analysis of the flow density field has been an important research direction of the flow field [1].

At present, the complex flow field parameter measurement technologies in wind tunnel tests mainly include schlieren and shadowgraph technology [2], interferometric length and phase-change measurement [3], and wave surface sensor technology [4]. However, there still exist some drawbacks in these technologies: schlieren and shadowgraph technology can merely do a qualitative analysis of the projection field density. The high-resolution interferometric system based on the interferometric length and phase-change measurement is very expensive. Meanwhile, it is vulnerable to external environmental disturbance, and the data post-processing technology is complex. Wave surface sensor has extensive applications in density analysis, but its spatial resolution is always limited by the dimensions of the microlens. To address these problems, Zhou et al. [5] proposed a video measurement method for the flow density field of the wind tunnel test model which provides a new method for the quantitative analysis of the density projection field. This method combines the background oriented schlieren (BOS) technology [6, 7] and video measurement technology to research the density projection field in the experiment. Consequently, through analysis and modeling, the



Content from this work may be used under the terms of the [Creative Commons Attribution 3.0 licence](https://creativecommons.org/licenses/by/3.0/). Any further distribution of this work must maintain attribution to the author(s) and the title of the work, journal citation and DOI.

relationship between the corresponding position of the flow field and its value can be established by a Poisson equation with source terms which has no analytical solution. Then the density projection field can be calculated by solving the Poisson equation.

Considering the problem that the Poisson equation does not have the analytical solution, a numerical method, which is based on the Finite element method (FEM) [8], is proposed. Meanwhile, instead of an analytical solution, the source term of the equation is a series of discrete points obtained by the measuring system, which makes it impossible to solve the equation directly by the FEM. To overcome the challenge, we first establish the fitting formula between the discrete points in the source terms and their corresponding coordinates. Compared with the previous fitting methods (i.e. surface fitting, interpolation, and back-propagation (BP) neural network), the method based on combined Genetic algorithms (GA) and BP neural network can achieve higher precision. Therefore, the paper mainly uses the GA-BP [9] network optimizing arithmetic to realize the high precision fitting.

2. Model Building of Density Projection Field

The density projection field is modeled by combining BOS technology and video measurement technology. In this system, figure 1 presents that the observation object of the camera is set as a background with lattice which is evenly distributed. When there is a disturbed flow field between the camera and the background, the imaging of every point in the lattice will generate a certain offset compared to the imaging without disturbed flow field [10], as shown in Figure 2. According to these offsets, we can calculate their corresponding offset angle ε_x and ε_y which are directly related to the density distribution ρ of the flow field [11]. And it can be described as follows:

$$\varepsilon_x = \frac{K_{GD}}{1 + K_{GD}\rho_0} \frac{\partial \rho}{\partial x} L, \quad \varepsilon_y = \frac{K_{GD}}{1 + K_{GD}\rho_0} \frac{\partial \rho}{\partial y} L \quad (1)$$

where the value of K_{GD} is $0.226 \text{ cm}^3/\text{g}$ under the standard air condition and ρ_0 is total pressure of the flow field. To obtain the Poisson equation [12] with source term, differential processing and adding operation are carried out on Equation (1). And the Poisson equation is as follows:

$$\frac{\partial^2 \rho}{\partial x^2} + \frac{\partial^2 \rho}{\partial y^2} = \frac{1 + K_{GD}\rho_0}{K_{GD}} \left(\frac{\partial \varepsilon_x}{\partial x} + \frac{\partial \varepsilon_y}{\partial y} \right) \quad (2)$$

Equation (2) presents the distribution of the density projection field. In this paper, we will calculate it by utilizing our proposed method.

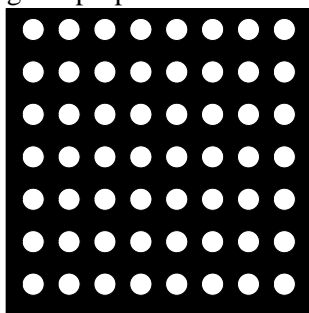


Figure 1. Standard plate with evenly distributed dots.

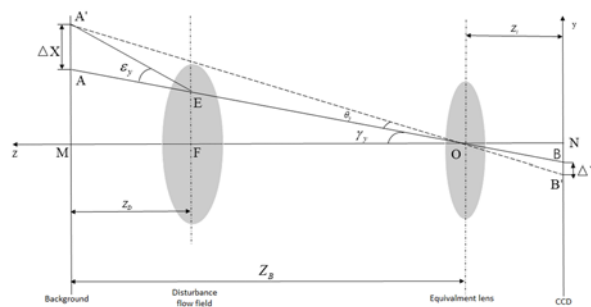


Figure 2. Optical path diagram of BOS system

3. Solution Process of Density Field

3.1. Triangle Mesh Division Method

As shown in figure 3, the area of the density projection field is discretized by adopting the triangle mesh division which can solve the Poisson equation more accurately based on FEM. And in the whole process of mesh partition, there are mainly three steps. Firstly, we divide the entire area into a number of rectangular grids according to the interval h . Then all the divided rectangular grids are diagonally

divided into a series of triangular elements. Finally, each triangle element and its corresponding vertices are numbered in order for the subsequent FEM solution [13].

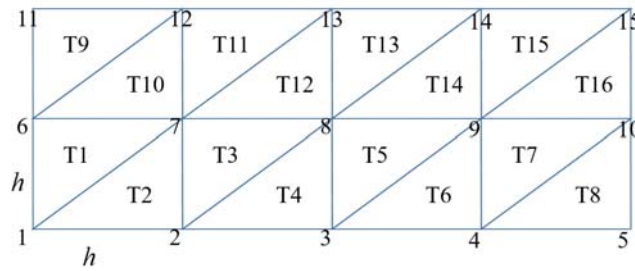


Figure 3. The area after using triangle mesh division method

3.2. Fitting of the Offset Angles

As shown previously, the source term of Equation (2) has no analytic function and we can merely calculate a set of discrete values that represent the offset angles. Therefore, it is essential to establish a fitting equation between the discrete points and their corresponding coordinates before we solve the Poisson equation by employing FEM. Meanwhile, as an important part of our proposed method, the accuracy of fitting directly determines the solving precision of the equation which makes us need to propose a fitting strategy with excellent performance.

In our method, we deploy the GA-BP neural network [9] to obtain the fitting equation between the offset angle and their corresponding coordinates x and y . As shown in figure 4, there are 3 full connection layers in the BP neural network. The coordinates x and y are used as the network for training and the offset angle as output. Then we use Adam optimizer with an initial learning rate of 0.1. Also, we choose MSE to measure the difference between the ground truth and the estimated value the network generated. What's more, before the training of the network, GA is utilized to find appropriate weights for the neural network which can greatly improve the fitting precision.

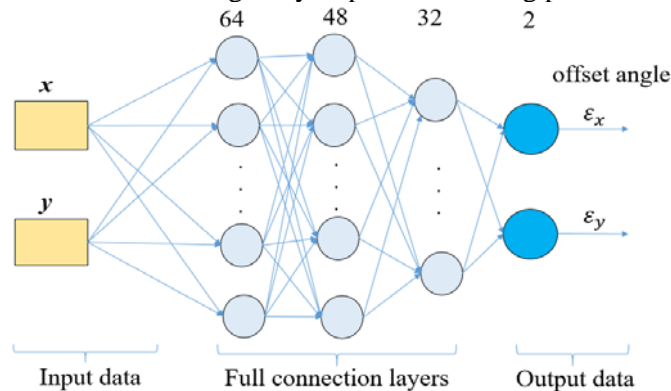


Figure 4. The structure diagram of BP neural network

A network model can be obtained after the network training finished. Then these vertex coordinates of triangulation are input into the model, and we can get their corresponding offset angles ϵ_x and ϵ_y . Equation (2) presents that the differential and adding operations are adopted to calculate the source terms $\frac{\partial \epsilon_x}{\partial x} + \frac{\partial \epsilon_y}{\partial y}$. And the five-point Equations for partial derivatives play a key role which can be expressed as follows:

$$\frac{\partial \epsilon_x}{\partial x} = \frac{4}{3h} * \left[net_{\epsilon_x} \left(x + \frac{h}{2}, y \right) - net_{\epsilon_x} \left(x - \frac{h}{2}, y \right) \right] - \frac{1}{6h} * \left[net_{\epsilon_x} \left(x + h, y \right) - net_{\epsilon_x} \left(x - h, y \right) \right]$$

$$\frac{\partial \epsilon_y}{\partial y} = \frac{4}{3h} * \left[net_{\epsilon_y} \left(x, y + \frac{h}{2} \right) - net_{\epsilon_y} \left(x, y - \frac{h}{2} \right) \right] - \frac{1}{6h} * \left[net_{\epsilon_y} \left(x, y + h \right) - net_{\epsilon_y} \left(x, y - h \right) \right] \quad (3)$$

where h denotes the interval of finite element mesh and net is the network model.

3.3. Solution of the Equation

When the Poisson equation is solved by FME, it will eventually be converted into the solution of linear systems of equations described as follows:

$$KU = F \quad (4)$$

where K is the global stiffness matrix, F is the nodal loads vector and U denotes the density projection field that needs to be solved. Therefore, we need to calculate the F and K before solving the linear equations. Similarly to many previous works, we can easily obtain the global stiffness matrix K by calculating the element stiffness matrix. However, during the calculation of the load vectors of elements, the calculation process is complicated and there exists some challenge. In the process, the double integrals are deployed after the coordinate transformation and it is expressed as follows:

$$f_i = \iint_{\Delta} g(x(\lambda_1, \lambda_2), y(\lambda_1, \lambda_2)) \lambda_i |J| d\lambda_1 d\lambda_2 \quad , i = 1, 2, 3 \quad \{(\lambda_1, \lambda_2) | 0 \leq \lambda_1 \leq 1 - \lambda_2, 0 \leq \lambda_2 \leq 1\} \quad (5)$$

$$g(x, y) = \frac{1 + K_{GD}\rho_0}{K_{GD}} \left(\frac{\partial \varepsilon_x}{\partial x} + \frac{\partial \varepsilon_y}{\partial y} \right), \quad |J| = \begin{vmatrix} \frac{\partial \lambda_1}{\partial x} & \frac{\partial \lambda_1}{\partial y} \\ \frac{\partial \lambda_2}{\partial x} & \frac{\partial \lambda_2}{\partial y} \end{vmatrix} \quad (6)$$

where the f_i denotes the interaction between the i_{th} shape function and source terms, $g(x, y)$ is the source term of the Poisson equation, $(x(\lambda_1, \lambda_2), y(\lambda_1, \lambda_2))$ are the transformed coordinates of the points on the elements, and $|J|$ is the Jacobian determinant of element transformation.

It is obvious that the $g(x, y)$ will be called multiple times when we calculate the f_i by using software. Also, it means that the neural network model will also be called many times, resulting in a serious reduction of calculation efficiency. Inspired by the infinitesimal dividing method, we replace the function surface of the whole triangle element with the plane determined by the function value of the node coordinate, as shown in Figure 5. Then we can employ the three nodes of triangular element and their corresponding source term values (x_1, y_1, z_1) , (x_2, y_2, z_2) and (x_3, y_3, z_3) to calculate the plane equation and it can be described as follows:

$$\begin{aligned} Ax + By + Cz + D &= 0 \\ \begin{cases} A = (y_3 - y_1)(z_3 - z_1) - (z_2 - z_1)(y_3 - y_1) \\ B = (x_3 - x_1)(z_3 - z_1) - (z_3 - z_1)(x_2 - x_1) \\ C = (x_2 - x_1)(y_2 - y_1) - (x_3 - x_1)(y_2 - y_1) \\ D = -(Ax_1 + By_1 + Cz_1) \end{cases} \end{aligned} \quad (7)$$

After that we rearrange the Equation (5) by utilizing the Equation (7), and the new generated equation can be described as follows:

$$f_i = \iint_{\Delta} \left[-\frac{A}{C}x(\lambda_1, \lambda_2) - \frac{B}{C}y(\lambda_1, \lambda_2) - \frac{D}{C} \right] \lambda_i |J| d\lambda_1 d\lambda_2 \quad , i = 1, 2, 3 \quad \{(\lambda_1, \lambda_2) | 0 \leq \lambda_1 \leq 1 - \lambda_2, 0 \leq \lambda_2 \leq 1\} \quad (8)$$

In this way, the neural network model will be called less often during the calculation of the load vectors of elements. Then the nodal loads vector F can be formulated more efficiently. Eventually, the projection density filed will be calculated by using K and F .

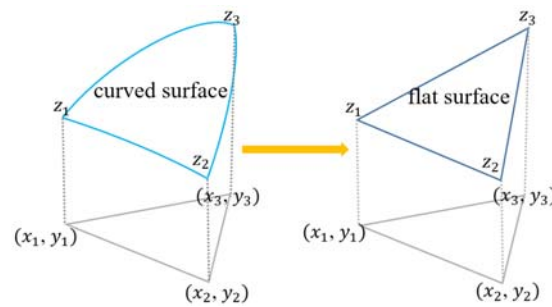


Figure 5. Treat the curved surface as the flat surface

4. Experimental Results

In this section, we evaluate the performance of the proposed method, the flow density field solution based on FEM, in terms of calculation accuracy and time efficiency. Firstly, we compared the fitting effects of the GA-BP neural network and the previous fitting methods on the source terms of the same equation. Then a simulation experiment was designed to compare the performance that the FEM and the proposed method can achieve. Furthermore, we utilized the offset angle data measured by the BOS system to prove the validity of the proposed method. Throughout this paper, all experiments are conducted with MATLAB R2018a on the desktop computer installed with 64-bit Windows 10 operating system.

4.1. The Comparison of Fitting Precision

We introduce a Poisson equation which has a theoretical analytical solution to verify that the fitting accuracy of the GA-BP neural network is higher than previous fitting methods. The equation can be described as follows:

$$\begin{cases} -\left(\frac{\partial^2 u}{\partial x^2} + \frac{\partial^2 u}{\partial y^2}\right) = g_1(x, y) \\ u|_{\partial\Omega} = 0 \end{cases} \quad (9)$$

$$\Omega = (0,10)^2, g_1(x, y) = -6x-6y, u(x, y) = x^3 + y^3$$

where the Ω is the definition field of the equation, $g_1(x, y)$ is the source term of the equation and $u(x, y)$ is the theoretical analytical solution of the equation. 5000 samples like $(x_n, y_n, g_{1n}(x_n, y_n))$ are obtained by random sampling from the source terms. Then the network is trained using the sampled data. After that, we perform the mesh generation in the definition field with different intervals h , and the source terms value of grid cell node are predicted by several methods. Meanwhile, L2 norm are used for error estimation and the formula is described as follows:

$$E_{L_2} = \|U - U_h\|_{L_2} = \sqrt{\sum_{i=0}^t \sum_j \left\{ |g'_{ij} - g_{ij}|^2 \right\} \times h_x \times h_y} \quad (10)$$

Table 1 shows the prediction error by using three approaches, respectively. It can be concluded that the smaller the interval h of mesh generation, the fitting error will be reduced. Meanwhile, the prediction error of GA-BP neural network is much lower than other fitting methods.

Table 1. The error comparison of fitting methods, the sample size the reciprocal if intervals h .

Sample size	Interpolation	BP	GA-BP
20×20	2.842104	0.012052	0.004819
40×40	1.102039	0.010243	0.006548
60×60	0.683544	0.009763	0.005953
80×80	0.495411	0.011239	0.005015
100×100	2.842104	0.010121	0.004819

4.2. The Simulation Experiment

Instead of exact analytical expressions, the BOS system merely measures a series of discrete offset angles. And we can not find the analytic solution of the Poisson equation. Therefore, by estimating the performance of accuracy and time consuming, we verify the effectiveness of our proposed method by utilizing Equation (11) which can be expressed as follows:

$$\begin{cases} -\left(\frac{\partial^2 u}{\partial x^2} + \frac{\partial^2 u}{\partial y^2}\right) = g_2(x, y) \\ u|_{\partial\Omega} = 0 \end{cases} \tag{11}$$

$$\Omega = (0,1)^2, g_2(x, y) = 2\pi^2 \sin \pi x \sin \pi y, u(x, y) = \sin \pi x \sin \pi y$$

In the experiment, we use the same data sampling method as in the BOS system to generate samples like $(x_n, y_n, g_{2n}(x_n, y_n))$ from the source terms. And the neural network is trained through these samples to replace the source term $g_2(x, y)$ shown in Equation (11). Then Equation (11) is solved by the FEM and our proposed method.

The error of the node z in the uniform finite element mesh can be defined as follows:

$$(u - u_h)(z) = w(z)h^2 + O(h^4) \tag{12}$$

Where u is the corresponding exact solution of z , u_h is the appropriate approximate solution when the element interval is h . when we change the interval h into half of the original, the error can be described as follows:

$$(u - u_{h/2})(z) = w(z)h^2 / 4 + O(h^4) \tag{13}$$

Consequently, we can deduce from Equation (12) and Equation (13) that the corresponding computable error of the interval $h/2$ is expressed as follows:

$$(u - u_{h/2})(z) = (u_{h/2} - u_h) / 3 + O(h^4) \tag{14}$$

For different intervals h , we compare the computable error of the proposed method with the original FME. Meanwhile, we compare the execution time of the two methods and the results are shown in Table 2. And the results and computable errors of our proposed method are shown in Figure 5.

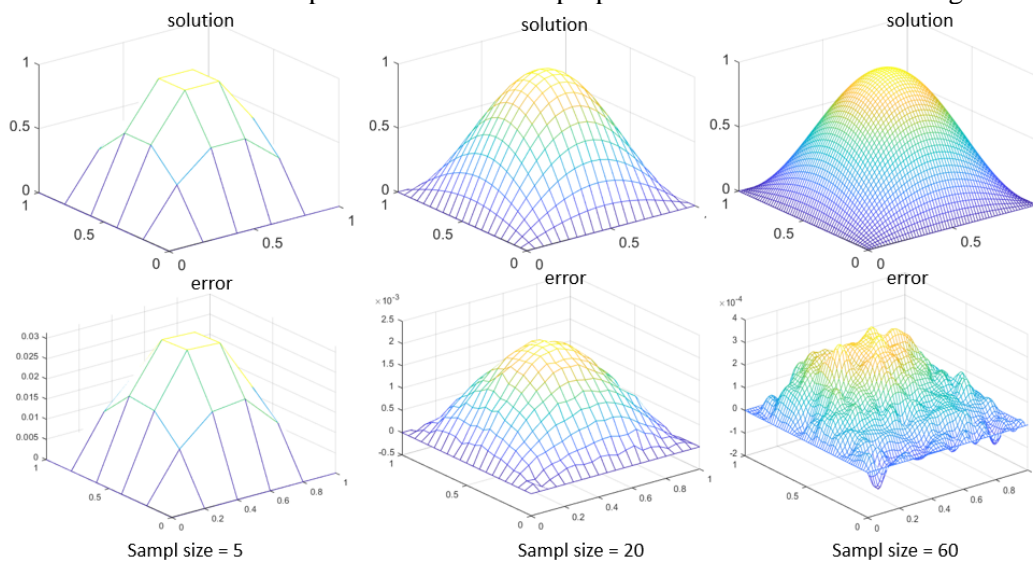


Figure 5. Solution and errors of our proposed method

Table 2. Error and time consuming of the two methods the sample size the reciprocal if intervals h .

Sample size	FEM		Our method	
	error	time (s)	error	time (s)
5×5	2.5900e-2	236.31	7.1000e-3	223.41
10×10	7.3000e-3	251.42	1.3000e-3	223.59
20×20	1.9000e-3	386.48	3.6282e-4	226.71
40×40	4.6523e-4	812.11	7.8869e-5	232.67
60×60	5.9298e-4	1590.92	6.7434e-5	246.94
80×80	3.8453e-4	2614.69	5.0443e-5	258.30

The difference between the two methods lies in the solution of the element load vector as discussed in section 3.3. Table 2 and Figure 5 show that the denser the mesh is, the smaller the computable error that the two methods can achieve. When the grid density reaches a certain degree, the computable error will not decrease any more. Meanwhile, our proposed method is not much different from the FEM in solution accuracy, but the time consuming is significantly reduced.

4.3. Solution of Density Projection Field

We get the discrete offset angles of source term through BOS system and solve the Equation (2) to calculate the density projection field, as shown in Figure 6. Meanwhile, according to these discrete data, The BOS system can quantitatively analyze the projected density field, and the result is illustrated in Figure 7.

Figure 5 presents that there are two main peaks in the projected density field, one is about 0.7 times of the ρ_0 and the other one is about 1.25 times of the ρ_0 . It shows that the solution result of the proposed method is basically consistent with the experimental result, which proves its effectiveness.

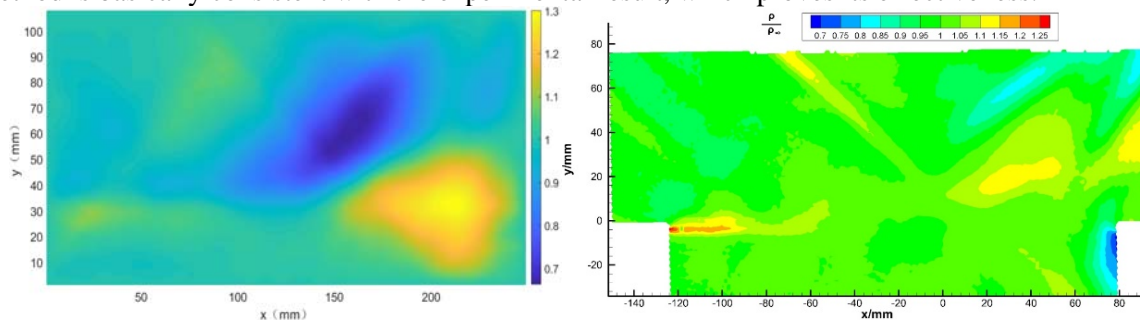


Figure 6. The result of the proposed method **Figure 7.** The result of BOS system

5. Conclusion

The source terms, which is composed of discrete points, poses great challenge for the solution of the Poisson equation. Our proposed improved FEM method provides a fast algorithm for it, and numerical simulation results show its high accuracy. By using the improved FEM method, the real experiment shows that the new scheme is very effective for the solution of density projection field. Therefore, it will be a good choice for the solution of density projection field.

Acknowledgement

This work was supported by the National Natural Science Foundation of China (11872069).

References

- [1] Zhang J, Xu D, Zhang L. “Research on density measurement based on background oriented schlieren method”, *Shiyan Liuti Lixue/journal of Experiments in Fluid Mechanics*, Vol. 29, No. 1, pp. 77-82, 2015.
- [2] Settles G S, Hargather M J. “A review of recent developments in schlieren and shadowgraph techniques”, *Measurement Science and Technology*, Vol. 28, No. 4, pp. 2017.

- [3] A Titov, I Malinovsky, H Belaïdi. “Precise interferometric length and phase-change measurement of gauge blocks based on reproducible wringing”, *Applied optics*, Vol. 39, No. 4, pp. 2000.
- [4] Ruile, Werner, Scholl, Gerd, Ostertag, Thomas, “Radio-interrogated surface-wave technology sensor”, Vol. No. pp. 2003.
- [5] ZHOU R.et.al. “Video measurement method of density projection field around wind tunnel test model”, Vol. No. pp. 2017.
- [6] Venkatakrisnan L, Meier G E A. “Density measurements using the Background Oriented Schlieren technique”, *Experiments in Fluids*, Vol. 37, No. 2 pp.237-247, 2004.
- [7] ZHANG Z Y, HUANG X H, YIN J, ZHOU R, LI D. “Research status and application of videogrammetric measurement techniques for wind tunnel testing”, *Acta Aerodynamica Sinica*, Vol. 37, No. 01 pp.70-79, 2016.
- [8] Zhiqiang, Cai, Seokchan, et al. “A finite element method using singular functions for the Poisson equation: crack singularities”, *Numerical Linear Algebra with Applications*, Vol. No. pp. 2002.
- [9] Song Y, Shen Y, Zhang G. “The information security risk assessment model based on GA – BP”, *ICSESS*, Vol. No. pp. 2016.
- [10] ZOU Y F. “Research of flow structure by video measurement technology”, *Mianyang: Southwest university of science and technology*, Vol. No. pp. 2019
- [11] ZHAO Y X, YI S H, TIAN L F, HE L, CHEN Z Y. “Aero-optic distortion and jitter of supersonic mixing layer—BOS measurement technology and its application”. *Scientia Sinica: Physica Mechanica Astronomica*, Vol. 40, No. 01, pp. 33-46, 2010.
- [12] GAO L, XU D. “Refractive index field measurement of random medium based on background oriented schlieren”. *Journal of Aerospace Power*, Vol. 32, No. 11, pp. 2653-2658, 2017.
- [13] Abreu E, Diaz C, Galvis J, et al. “On high-order conservative finite element methods”, *Computers & mathematics with applications*, Vol. 75, No. 6, pp. 1852-1867, 2018.